

Supplemental information

**Engineered human cytokine/antibody fusion proteins
expand regulatory T cells and confer
autoimmune disease protection**

Derek VanDyke, Marcos Iglesias, Jakub Tomala, Arabella Young, Jennifer Smith, Joseph A. Perry, Edward Gebara, Amy R. Cross, Laurene S. Cheung, Arbor G. Dykema, Brian T. Orcutt-Jahns, Tereza Henclová, Jaroslav Golias, Jared Balolong, Luke M. Tomasovic, David Funda, Aaron S. Meyer, Drew M. Pardoll, Joanna Hester, Fadi Issa, Christopher A. Hunter, Mark S. Anderson, Jeffrey A. Bluestone, Giorgio Raimondi, and Jamie B. Spangler

Figure S1

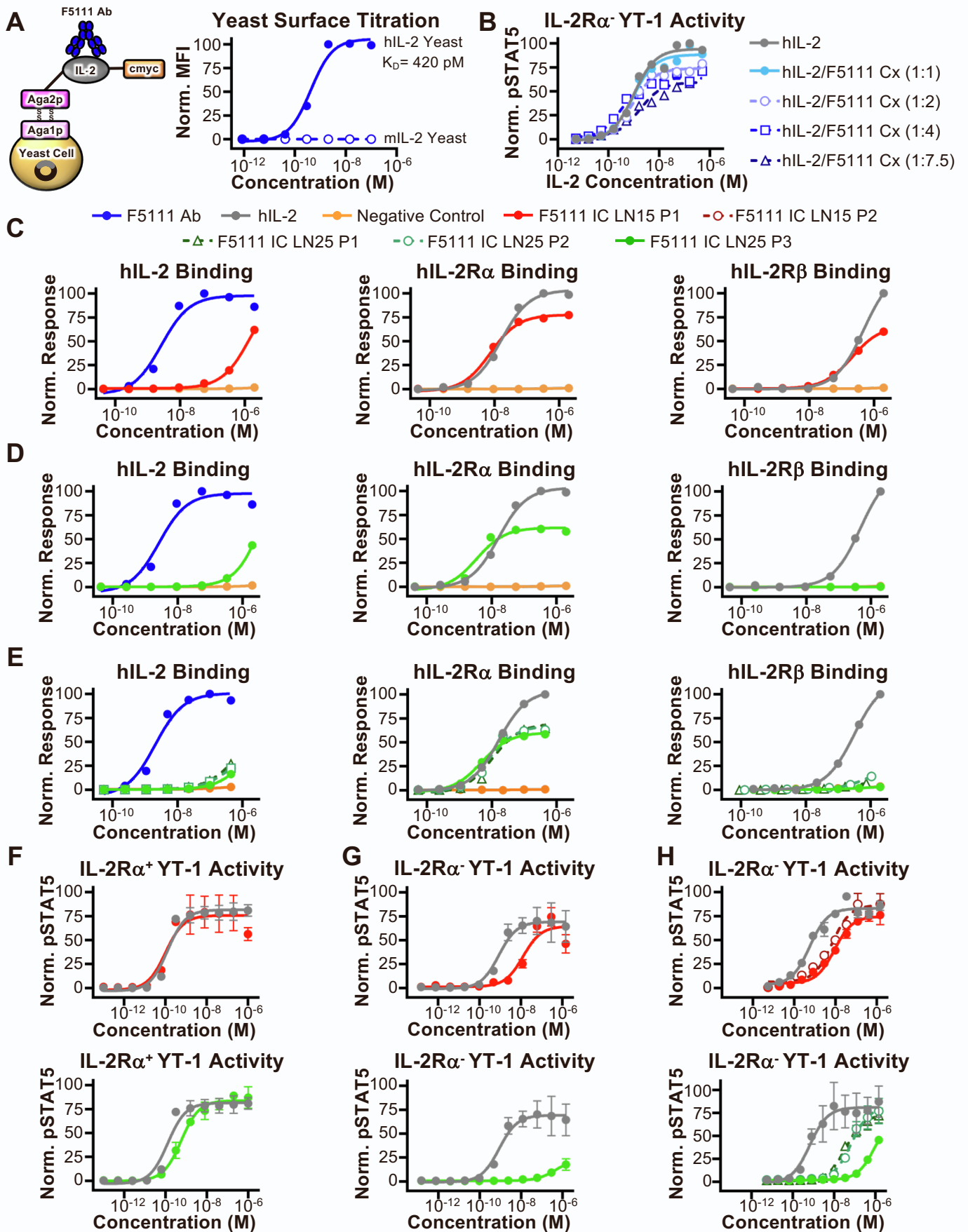
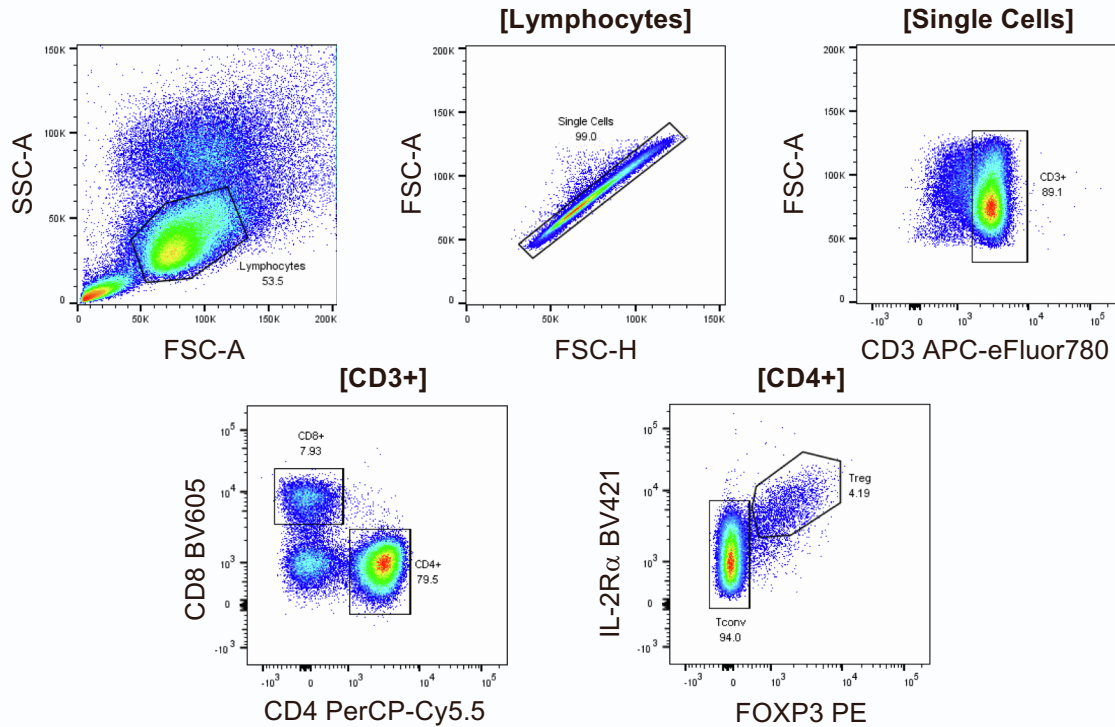


Figure S1. Increasing IC linker length improves Treg bias. Related to Figures 1 and 2.

(A) Binding of the F5111 antibody (Ab) to yeast-displayed hIL-2 or mL-2. Fitted equilibrium dissociation constant (K_D) is shown. **(B)** STAT5 phosphorylation response of IL-2R α^- YT-1 human NK cells stimulated with either hIL-2 or hIL-2/F5111 complex (Cx) at varying molar ratios of cytokine to antibody. **(C-E)** Equilibrium biolayer interferometry-based titrations of hIL-2, F5111 antibody (Ab), Negative Control (trastuzumab), F5111 IC LN15 P1, and F5111 IC LN25 P1, P2, and P3 binding to immobilized hIL-2 (left), immobilized hIL-2R α (middle), and immobilized hIL-2R β (right). **(F)** STAT5 phosphorylation response of IL-2R α^+ YT-1 human NK cells stimulated with either hIL-2, F5111 IC LN15 P1 (top), or F5111 IC LN25 P3 (bottom). **(G)** STAT5 phosphorylation response of IL-2R α^- YT-1 human NK cells stimulated with either hIL-2, F5111 IC LN15 P1 (top), or F5111 IC LN25 P3 (bottom). **(H)** STAT5 phosphorylation response of IL-2R α^- YT-1 human NK cells stimulated with either hIL-2, F5111 IC LN15 P1 and P2 (top), or F5111 IC LN25 P1, P2, and P3 (bottom). Data in **(F-H)** represent mean \pm SD (n=3). See also **Tables S2 and S3**.

Figure S2

A



B

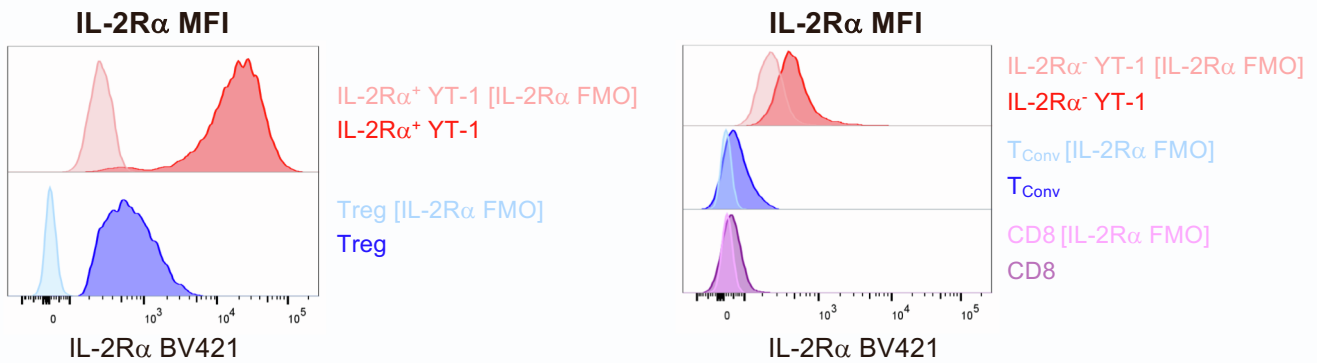


Figure S2. IL-2R α ⁺ YT-1 cells express higher levels of IL-2R α than human Tregs. Related to Figures 2, 3, and 5. (A) Representative flow cytometry plots illustrating the gating strategy used for human PBMCs. **(B)** Representative histograms illustrating IL-2R α MFI of IL-2R α ⁺ YT-1 cells and human Tregs (left) and IL-2R α ⁻ YT-1 cells, human CD8⁺ T cells, and human T_{Conv} cells (right) as compared to the IL-2R α fluorescence minus one (FMO) controls.

Figure S3

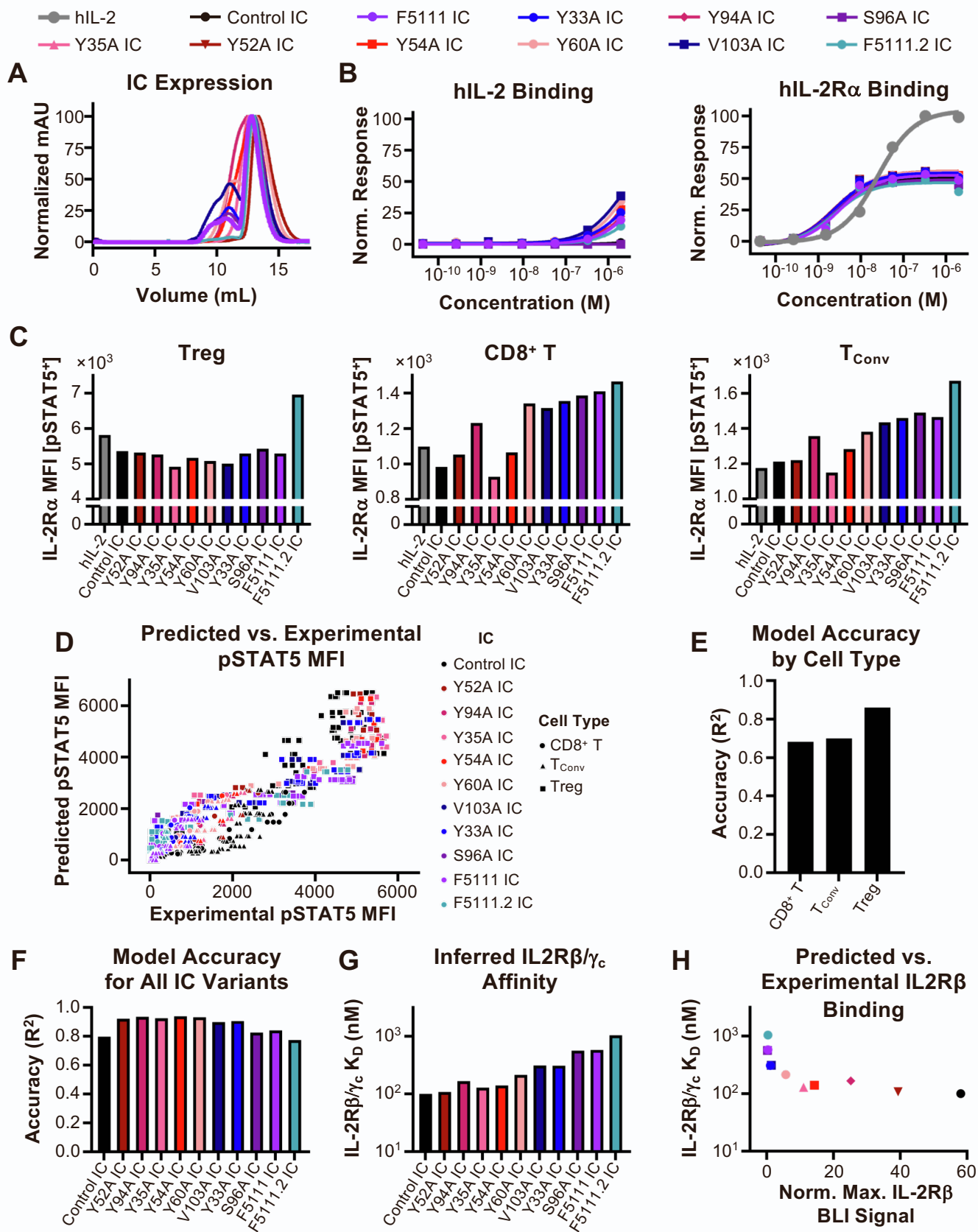


Figure S3. Characterization of F5111 IC variants. Related to Figures 3 and 4. (A) Overlay of SEC traces for F5111 IC variants. **(B)** Equilibrium biolayer interferometry-based titrations of hIL-2, Control IC, and F5111 IC variants binding to immobilized hIL-2 (left) and immobilized hIL-2R α (right). Binding to immobilized hIL-2 was normalized based on the binding of the F5111.2 antibody (**Figure S5C, left**). **(C)** IL-2R α MFI within the pSTAT5⁺ population of Treg (left), CD8⁺ T (middle), and T_{Conv} (right) cell populations within human PBMCs stimulated with either hIL-2, Control IC, or F5111 IC variants at treatment concentrations of 2 nM (left) and 200 nM (middle and right). **(D)** Predicted vs. experimentally measured pSTAT5 MFI for all cell types, ICs, and concentrations modeled. Each point represents a single experimental measurement (n=1). **(E)** Model accuracy delineated by cell type for all ICs. **(F)** Model accuracy delineated by treatment for all ICs. Accuracies are calculated as a Pearson's correlation R². **(G)** Inferred IL2R β / γ_c equilibrium dissociation constants (K_D, nM) for each IC. **(H)** Inferred IL2R β / γ_c equilibrium dissociation constants (K_D, nM) compared to the maximum normalized IL2R β biolayer interferometry (BLI) signal experimentally measured for each IC. See also **Table S2**.

Figure S4

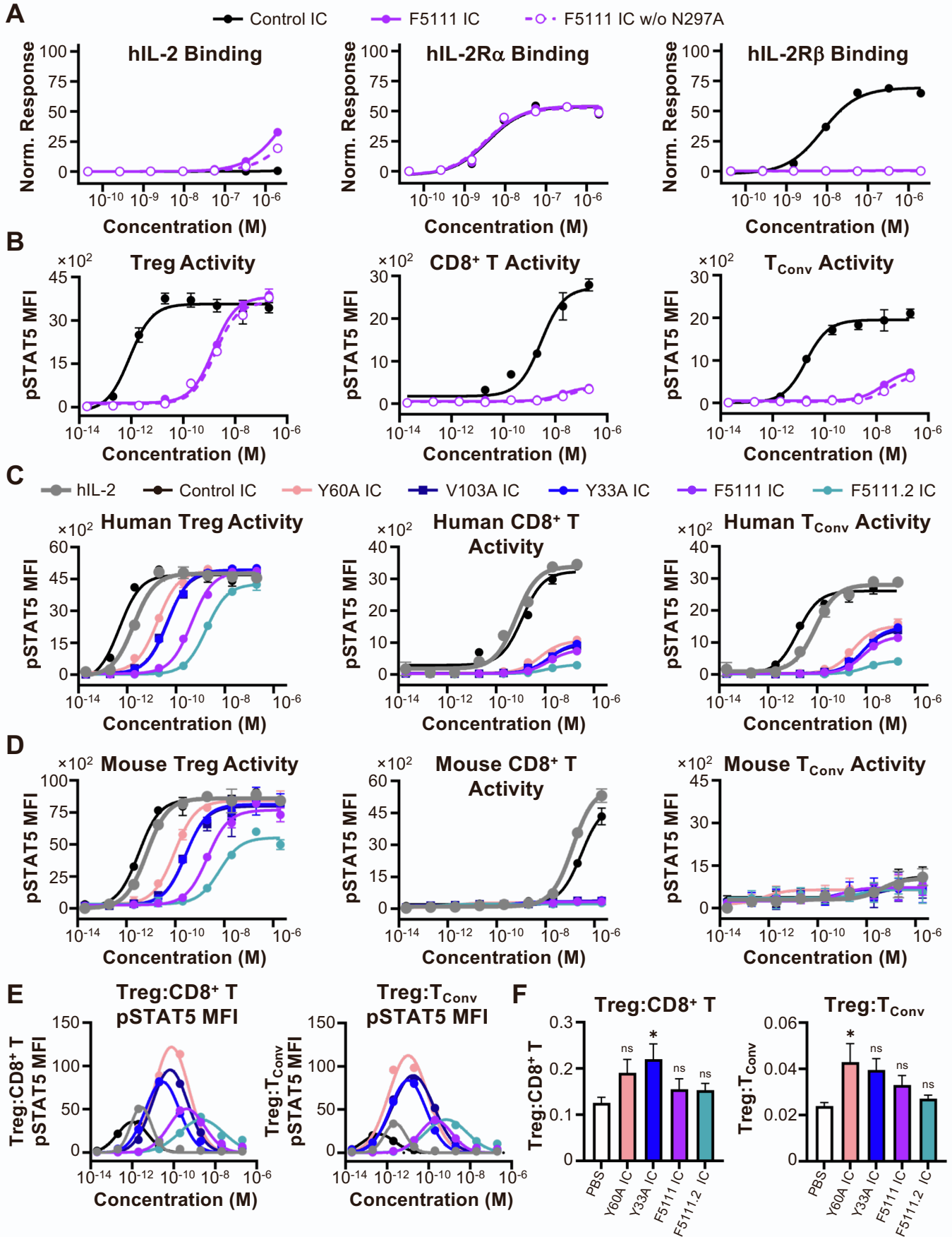


Figure S4. The N297A mutation does not impact *in vitro* function and IC variants modulate Treg bias *in vitro* and *in vivo*. Related to Figures 3 and 4. (A) Equilibrium biolayer interferometry-based titrations of Control IC, F5111 IC, and F5111 IC without the N297A mutation (w/o N297A, intact effector function) binding to immobilized hIL-2 (left), immobilized hIL-2R α (middle), and immobilized hIL-2R β (right). Binding to immobilized hIL-2 was normalized based on the binding of the F5111.2 antibody (**Figure S5C, left**). **(B)** STAT5 phosphorylation response of Treg (left), CD8⁺ T (middle), and T_{Conv} (right) cell populations from human PBMCs stimulated with either Control IC, F5111 IC, or F5111 IC w/o N297A. Data represent mean \pm SD (n=3). **(C)** STAT5 phosphorylation response of Treg (left), CD8⁺ T (middle), and T_{Conv} (right) cell populations within human PBMCs stimulated with either hIL-2, Control IC, Y60A IC, V103A IC, Y33A IC, F5111 IC, or F5111.2 IC (all with N297A mutation). Data represent mean \pm SD (n=3). **(D)** STAT5 phosphorylation response of Treg (left), CD8⁺ T (middle), and T_{Conv} (right) cells isolated from spleens of NOD mice and stimulated with either hIL-2, Control IC, Y60A IC, V103A IC, Y33A IC, F5111 IC, or F5111.2 IC (all with N297A mutation). Data represent mean \pm SD (n=3). **(E)** Average pSTAT5 MFI ratio of human Treg:CD8⁺ T (left) and human Treg:T_{Conv} (right) for each IC determined at each stimulation concentration from the experiment shown in **(C)**. **(F)** BRG mice were administered 5×10^6 human PBMCs (*i.p.*) on day 0 and then on day 1 were treated (*i.p.*) with either PBS (n=6) or 8.2 μ g (1.5 μ g IL-2 equivalence) Y60A IC (n=5), Y33A IC (n=4), F5111 IC (n=4), or F5111.2 IC (n=5). Cells were collected by lavage from the peritoneum on day 4 and ratios of human Treg:CD8⁺ T (left) and Treg:T_{Conv} (right) were evaluated. Data represent mean + SEM. Statistical significance was determined by one-way ANOVA with a Tukey post hoc test. Only statistical significance compared to PBS is shown on the plots. All statistical data are provided in **Table S6**. *P \leq 0.05, **P \leq 0.01, ***P \leq 0.001, ****P \leq 0.0001. See also **Tables S2, S4, and S5**.

Figure S5

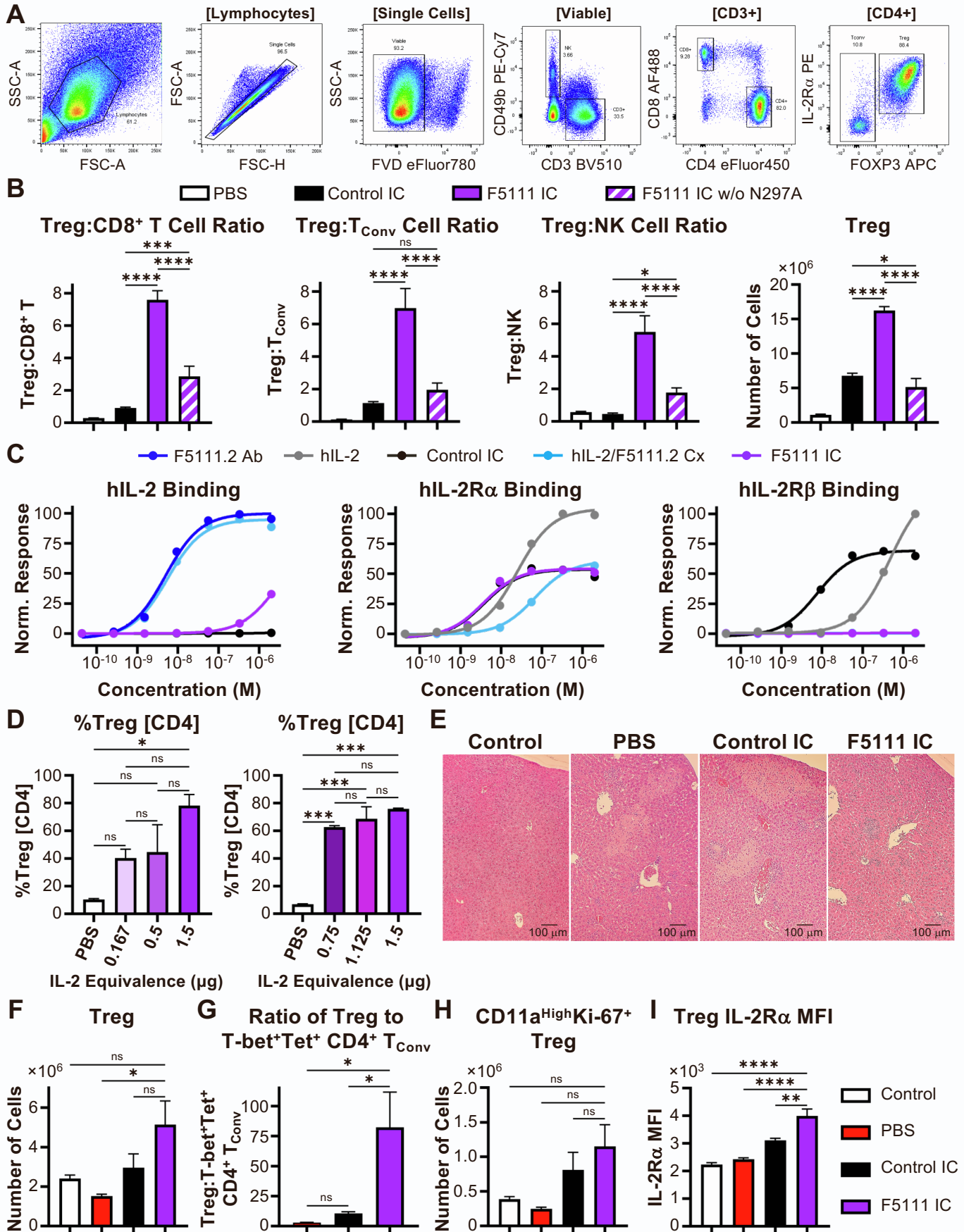


Figure S5. *In vivo* characterization of F5111 IC. Related to Figures 4-6. (A) Representative flow cytometry plots illustrating the gating strategy used for NOD mouse immune cell subset expansion studies. **(B)** Ratios of Treg to CD8⁺ T cells (left), Treg to T_{Conv} cells (middle), and Treg to NK cells (right) in spleens harvested from NOD mice (n=4 per group) treated daily for four days (*i.p.*) with either PBS or 8.2 μg (1.5 μg IL-2 equivalence) Control IC, F5111 IC, or F5111 IC without the N297A mutation (w/o N297A, intact effector function). Data represent mean + SD. Statistical significance was determined by one-way ANOVA with a Tukey post hoc test. Significance is shown between Control IC and F5111 IC with and without the N297A mutation. **(C)** Equilibrium biolayer interferometry-based titrations of F5111.2 antibody (Ab), hIL-2, Control IC, hIL-2/F5111.2 complex (Cx, 1:1 molar ratio), and F5111 IC binding to immobilized hIL-2 (left), immobilized hIL-2R α (middle), and immobilized hIL-2R β (right). **(D)** C57BL/6 mice (n=2 per group) were treated daily for 4 days (*i.p.*) with either PBS or varying dosages of F5111 IC: 0.91 μg (0.167 μg IL-2 equivalence); 2.7 μg (0.5 μg IL-2 equivalence); 4.1 μg (0.75 μg IL-2 equivalence); 6.2 μg (1.125 μg IL-2 equivalence); or 8.2 μg (1.5 μg IL-2 equivalence). Spleens were harvested 24 hours after the last dose. Percent of Tregs within the CD4⁺ T cell population is shown. Data represent mean + SD. Statistical significance was determined by one-way ANOVA with a Tukey post hoc test. **(E-I)** C57BL/6 mice were administered (*i.p.*) 25 cysts of the ME-49 strain of *Toxoplasma gondii* (*T. gondii*) on day 0. Control group designates disease-free mice that were not given cysts. Starting on day 1, mice were treated daily for 5 days (*i.p.*) with either PBS (Control, n=5; PBS, n=4) or 8.2 μg (1.5 μg IL-2 equivalence) Control IC (n=5) or F5111 IC (n=5). Mice were sacrificed on day 10. **(E)** Representative H&E staining of harvested mouse livers. Scale bar, 100 μm. **(F)** Total number of Tregs in harvested spleen. **(G)** Ratio of Tregs to T-bet⁺Tetramer (Tet)⁺ CD4⁺ T_{Conv} cells in harvested mouse spleen. **(H)** Total number of CD11a^{High}Ki-67⁺ Tregs in harvested mouse spleen. **(I)** IL-2R α MFI of Tregs in harvested mouse spleen. Data in **(F-I)** represent mean + SEM. Statistical significance in **(F-I)** was determined by one-way ANOVA with a Tukey post hoc test. Significance compared to F5111 IC is shown. All statistical data are provided in **Table S6**. *P \leq 0.05, **P \leq 0.01, ***P \leq 0.001, ****P \leq 0.0001. See also **Table S2**.

Figure S6

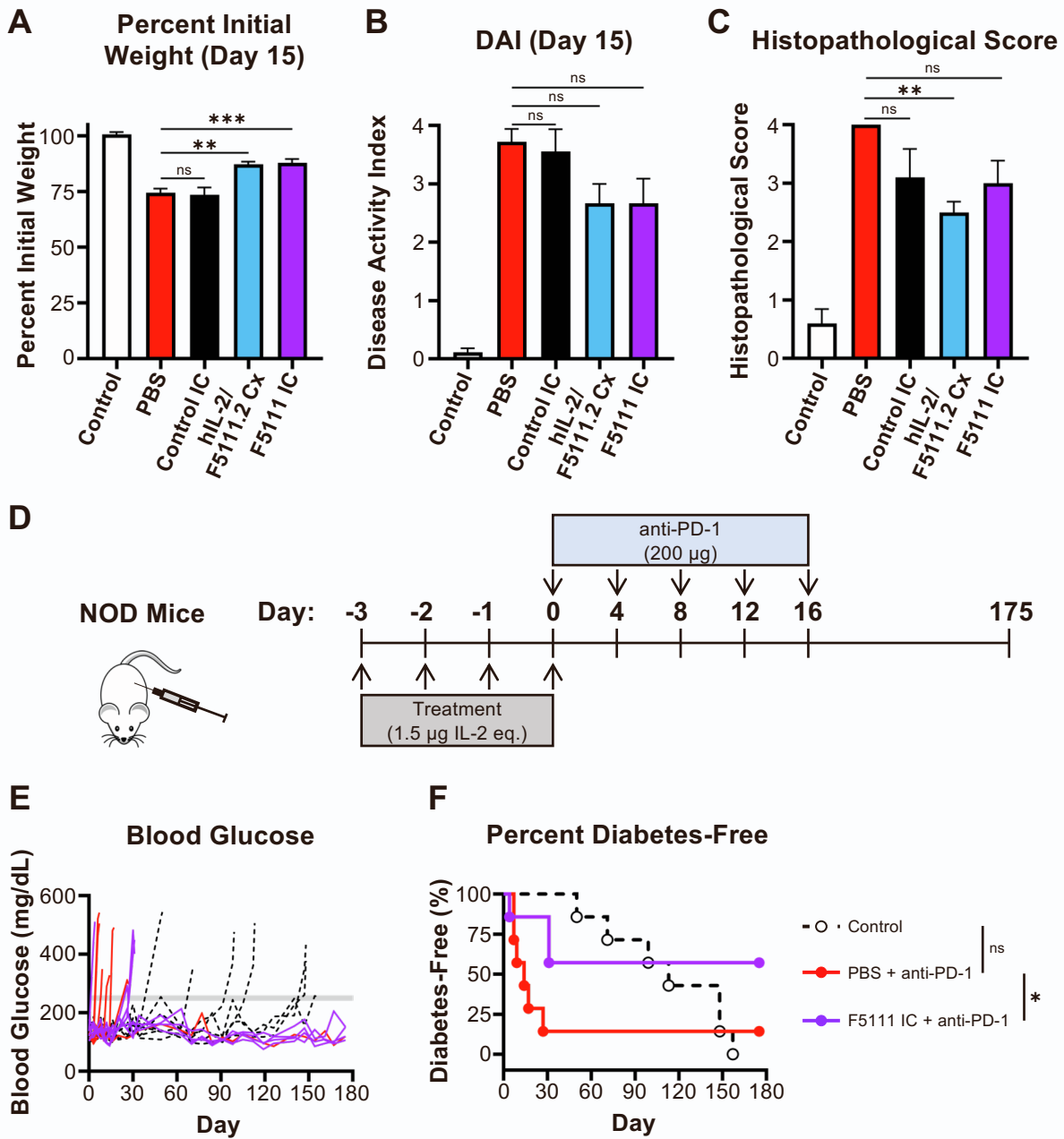


Figure S6. Evaluation of F5111 IC in mouse models of autoimmune disease. Related to Figure 7. (A-C) BALB/c mice (n=6 per group) were treated daily for 7 days (*i.p.*) with either PBS (Control and PBS), 1.5 μ g hIL-2 complexed with 6.6 μ g F5111.2 antibody (1:2 molar ratio, hIL-2/F5111.2 Cx), or 8.2 μ g (1.5 μ g IL-2 equivalence) Control IC or F5111 IC. Beginning on day 7, all groups except for the disease-free cohort (Control) were administered 3% DSS in their drinking water. Mice were sacrificed on day 15. **(A)** Weight change on day 15. **(B)** Disease activity index (DAI) on day 15. **(C)** Histopathology scores for H&E stained colons (n=5 Control, Control IC; n=6 PBS, Cx, F5111 IC). Data represent mean \pm SEM. Statistical significance was determined by one-way ANOVA with a Tukey post hoc test. All plots show significance of Control IC, Cx, and F5111 IC treated mice versus PBS treated mice. **(D-F)** 8-week-old NOD mice (n=7 per group) were treated daily for 4 days (*i.p.*, days -3, -2, -1, 0) with either PBS (Control and PBS) or 8.2 μ g (1.5 μ g IL-2 equivalence) F5111 IC. Starting on day 0 (4 hours after the last IC dose), mice were administered anti-PD-1 antibody (200 μ g) every 4 days until day 16. Control group designates mice that did not receive anti-PD-1 antibody. **(E)** Blood glucose concentrations over the study. The threshold 250 mg/dL value is indicated by the gray line. **(F)** Percent diabetes-free mice. Statistical significance was determined by pairwise comparisons using the Log-rank (Mantel-Cox) test. Statistical significance compared to mice treated with PBS + anti-PD-1 is shown. All statistical data are provided in **Table S6**. *P \leq 0.05, **P \leq 0.01, ***P \leq 0.001, ****P \leq 0.0001.

Table S1. Antibody and IC sequences. Related to Figures 1 and 3.

Construct	Amino Acid Sequence Signal sequence – V _H or V _L – human IgG1 C _H 1, C _H 2, and C _H 3 – hIL-2 – Linker – human Lambda C _L
F5111 Heavy Chain (Single-point alanine mutations) (N297A)	METDTLLLWVLLLWVPGSTGDQLQLQESGPGLVKPSQTLSTCTVSGGSISSGGYYWSWIR QHPGKGLEWIGYIYSGSTIYNPSLKSRTISVDTSKNQFSLKLSVTAADTAVYYCARTPTV TGDWFDWPWGRGTLVTVSSASTKGPSVFPLAPSSKSTSGGTAALGCLVKDYFPEPVTVSWN SGALTSGVHTFPAVLQSSGLYSLSSVTVPSSSLGTQTYICNVNHKPSNTKVDKKEPKSCD KTHTCPPCPAPELLGGPSVFLFPPKPKDTLMISRTPEVTCVVVDVSHEDPEVKFNWYVDGVE VHNAKTKPREEQYNSTYRVVSVLTVLHQDWLNGKEYKCKVSNKALPAPIEKTISKAKGQPRE PQVYTLPPSREEMTKNQVSLTCLVKGFYPSDIAVEWESNGQPENNYKTPPVLDSDGSFLL YSKLTVDKSRWQQGNVFCFSVMHEALHNHYTQKLSLSLSPGK
F5111 Light Chain	MRVPAQLLGLLLWLPGARCGSNFMLTQPHSVSESPGKTVTISCTRSSGSIASNYVQWYQQ RPGSSPTTVIYEDNQRPSGVPDRFSGSIDSSNSASLTISGLKTEDEADYYCQSYDSSNVVF GGGKTLTVLGQPKAAPSVTLPFPSSEELQANKATLVCLISDFYPGAVTVAWKADSSPVKAGV ETTPSKQSNKYAASSYLSTPEQWKSHRSYSCQVTHEGSTVEKTVAPTECS
F5111 Light Chain + hIL-2 LN15: X = 3 LN25: X = 5 LN35: X = 7 (Single-point alanine mutations)	MYRMQLLSCIALSLALVTNSAPTSSSTKKTQLQLEHLLLDLQMLNGINNYKNPKLTRMLTFKF YMPKKATELKHLCLEELKPLEEVLNLAQSKNFHLRPRDLISINIVIVLELKGSETTFMCEYA DETATIVEFLNRWITFCQSIISTLT(GGGGS) _x NFMLTQPHSVSESPGKTVTISCTRSSGSIASN YVQWYQQRPGSSPTTVIYEDNQRPSGVPDRFSGSIDSSNSASLTISGLKTEDEADYYCQS YDSNVVFGGGKTLTVLGQPKAAPSVTLPFPSSEELQANKATLVCLISDFYPGAVTVAWKAD SSPVKAGVETTPSKQSNKYAASSYLSTPEQWKSHRSYSCQVTHEGSTVEKTVAPTECS
Control IC Heavy Chain (N297A)	METDTLLLWVLLLWVPGSTGDQVQLVESGGNLVQPGGSLRLSCAASGFTFGSFSMSWVRQ APGGGLEWVAGLSARSSLTHYADSVKGRFTISRDNKNSVYLQMNSLRVEDTAVYYCARRS YDSSGYWGHFYSDVWVGGTGLTVSASTKGPSVFPLAPSSKSTSGGTAALGCLVKDYFP EPVTVSWNSGALTSGVHTFPAVLQSSGLYSLSSVTVPSSSLGTQTYICNVNHKPSNTKVDK KVEPKSCDKTHTCPPCPAPELLGGPSVFLFPPKPKDTLMISRTPEVTCVVVDVSHEDPEVKF FNWYVDGVEVHNAKTKPREEQYNSTYRVVSVLTVLHQDWLNGKEYKCKVSNKALPAPIEKT ISKAKGQPREPQVYTLPPSREEMTKNQVSLTCLVKGFYPSDIAVEWESNGQPENNYKTPPV LDSDGSFLLYSKLTVDKSRWQQGNVFCFSVMHEALHNHYTQKLSLSLSPGK
Control IC Light Chain + hIL-2	MYRMQLLSCIALSLALVTNSAPTSSSTKKTQLQLEHLLLDLQMLNGINNYKNPKLTRMLTFKF YMPKKATELKHLCLEELKPLEEVLNLAQSKNFHLRPRDLISINIVIVLELKGSETTFMCEYA DETATIVEFLNRWITFCQSIISTLTGGGGSGGGSGGGSGGGSGGGSGGGSGGGSGGGG SVLTVQSSVSAAPGQVTISCSGTSNIGNNYVSWYQQHPGKAPKLMYDVKRPSGVPD RFSGSKSGNSASLDISGLQSEDEADYYCAAWDDSLSEFLFGTGTKLTVLGGQPKAAPSVTLP FPSSEELQANKATLVCLISDFYPGAVTVAWKADSSPVKAGVETTPSKQSNKYAASSYLST TPEQWKSHRSYSCQVTHEGSTVEKTVAPTECS
F5111.2 Heavy Chain (N297A)	METDTLLLWVLLLWVPGSTGDQLQLQESGPGLVKPSQTLSTCTVSGGSISSGGYYWSWIR QHPGKGLEWIGYIYKSGSAYYSPSLKSRTISVDTSKNQFSLKLSVTAADTAVYYCARTPTV TGDWFDWPWGRGTLVTVSSASTKGPSVFPLAPSSKSTSGGTAALGCLVKDYFPEPVTVSWN SGALTSGVHTFPAVLQSSGLYSLSSVTVPSSSLGTQTYICNVNHKPSNTKVDKKEPKSCD KTHTCPPCPAPELLGGPSVFLFPPKPKDTLMISRTPEVTCVVVDVSHEDPEVKFNWYVDGVE VHNAKTKPREEQYNSTYRVVSVLTVLHQDWLNGKEYKCKVSNKALPAPIEKTISKAKGQPRE PQVYTLPPSREEMTKNQVSLTCLVKGFYPSDIAVEWESNGQPENNYKTPPVLDSDGSFLL YSKLTVDKSRWQQGNVFCFSVMHEALHNHYTQKLSLSLSPGK
F5111.2 Light Chain	MRVPAQLLGLLLWLPGARCGSNFMLTQPHSVSESPGKTVTISCTRSSGSIASNYVQWYQQ RPGSSPTTVIYEDNQRPSGVPDRFSGSIDSSNSASLTISGLKTEDEADYYCQYDSIDVYFG GGKTLTVLGQPKAAPSVTLPFPSSEELQANKATLVCLISDFYPGAVTVAWKADSSPVKAGV ETTPSKQSNKYAASSYLSTPEQWKSHRSYSCQVTHEGSTVEKTVAPTECS
F5111.2 Light Chain + hIL-2	MYRMQLLSCIALSLALVTNSAPTSSSTKKTQLQLEHLLLDLQMLNGINNYKNPKLTRMLTFKF YMPKKATELKHLCLEELKPLEEVLNLAQSKNFHLRPRDLISINIVIVLELKGSETTFMCEYA DETATIVEFLNRWITFCQSIISTLTGGGGSGGGSGGGSGGGSGGGSGGGSGGGSGGGG SNFMLTQPHSVSESPGKTVTISCTRSSGSIASNYVQWYQQRPGSSPTTVIYEDNQRPSGVP DRFSGSIDSSNSASLTISGLKTEDEADYYCQYDSIDVYFGGGKTLTVLGQPKAAPSVTLP PSSEELQANKATLVCLISDFYPGAVTVAWKADSSPVKAGVETTPSKQSNKYAASSYLST PEQWKSHRSYSCQVTHEGSTVEKTVAPTECS

Table S2. Equilibrium K_D values from biolayer interferometry studies. Related to Figures 2 and 3.

Treatment	Equilibrium K_D (nM)			Figure
	hIL-2	hIL-2R α	hIL-2R β	
F5111 Ab	2.7	-	-	2A, S1C, S1D
hIL-2	-	16	480	2A, S1C, S1D
Control IC	-	3.4	4.4	2A
hIL-2/F5111 Complex	4.8	18	>2000	2A
F5111 IC LN35	>2000	3.0	>2000	2A
hIL-2	-	25	470	3B, S3B, S5C
Control IC	-	2.5	4.1	3B, S3B
F5111 IC	>2000	3.2	>2000	3B, S3B, S4A
Y33A IC	>2000	2.6	>2000	3B, S3B
Y94A IC	>2000	2.2	>2000	3B, S3B
S96A IC	>2000	2.5	>2000	3B, S3B
Y35A IC	>2000	2.5	>2000	3B, S3B
Y52A IC	>2000	2.8	500	3B, S3B
Y54A IC	>2000	2.8	>2000	3B, S3B
Y60A IC	>2000	2.7	>2000	3B, S3B
V103A IC	>2000	2.4	>2000	3B, S3B
F5111.2 IC	>2000	2.4	>2000	3B, S3B
F5111 IC LN15	>2000	7.5	210	S1C
F5111 IC LN25	>2000	3.4	>2000	S1D
F5111 Ab	2.1	-	-	S1E
hIL-2	-	16	310	S1E
F5111 IC LN25 P1	>2000	11	>700	S1E
F5111 IC LN25 P2	>2000	8.1	>1000	S1E
F5111 IC LN25 P3	>2000	4.8	>2000	S1E
Control IC + N297A	-	3.8	7.7	S4A, S5C
F5111 IC + N297A	>2000	3.6	>2000	S4A, S5C
F5111.2 Ab + N297A	4.9	-	-	S5C
hIL-2/F5111.2 Complex	5.6	68	>2000	S5C

**Table S3. EC₅₀ and E_{Max} Values from YT-1 cell activation studies.
Related to Figure 2.**

Treatment	EC ₅₀ (nM)		Normalized E _{Max}		Figure
	IL-2Rα ⁺	IL-2Rα ⁻	IL-2Rα ⁺	IL-2Rα ⁻	
hIL-2	0.13	0.88	82	69	2B, S1F, S1G
Control IC	0.031	0.83	87	91	2B
hIL-2/F5111 Complex	0.081	1.8	85	62	2B
F5111 IC LN35	0.70	>2000	80	21	2B
hIL-2	-	0.98	-	94	S1B
hIL-2:F5111 = 1:1	-	0.91	-	88	S1B
hIL-2:F5111 = 1:2	-	0.89	-	74	S1B
hIL-2:F5111 = 1:4	-	0.35	-	64	S1B
hIL-2:F5111 = 1:7.5	-	1.7	-	60	S1B
F5111 IC LN15	0.10	13	76	65	S1F, S1G
F5111 IC LN25	0.58	>2000	84	23	S1F, S1G
hIL-2	-	0.57	-	83	S1H (top)
F5111 IC LN15 P1	-	8.9	-	75	S1H
F5111 IC LN15 P2	-	6.9	-	87	S1H
hIL-2	-	0.68	-	81	S1H (bottom)
F5111 IC LN25 P1	-	37	-	73	S1H
F5111 IC LN25 P2	-	69	-	82	S1H
F5111 IC LN25 P3	-	>2000	-	76	S1H

**Table S4. EC₅₀ and E_{Max} values from human PBMC activation studies.
Related to Figures 2, 3, and 5.**

Treatment	EC ₅₀ (pM)			E _{Max} (pSTAT5 MFI)			Figure
	Treg	CD8 ⁺ T	T _{Conv}	Treg	CD8 ⁺ T	T _{Conv}	
hIL-2	4.5	1200	110	5300	3600	2500	2C
Control IC	1.3	1600	30	5200	3300	2400	2C
hIL-2/F5111 Complex	3.7	240	70	5100	2200	2200	2C
F5111 IC LN35	1700	6.1e4	3.7e4	5200	760	1100	2C
hIL-2	5.2	1000	110	5300	3500	2400	3C
Control IC	1.4	1500	39	5600	3600	2500	3C
F5111 IC	2100	5.0e4	3.4e4	5500	740	980	3C
Y33A IC	81	2.2e4	1.5e4	5300	1100	1400	3C
Y94A IC	6.9	4300	1200	5400	1800	1900	3C
S96A IC	910	3.3e4	2.6e4	5100	710	1000	3C
Y35A IC	7.7	4100	1400	5700	1800	2100	3C
Y52A IC	2.9	3500	360	5500	2300	2200	3C
Y54A IC	7.8	3000	1300	5500	1600	1900	3C
Y60A IC	15	5300	2900	5400	1400	1800	3C
V103A IC	51	1.3e4	7400	5300	1000	1400	3C
F5111.2 IC	8600	>2.0e5	>2.0e5	4700	370	460	3C
hIL-2	1.8	890	35	3700	2800	2100	5A
Control IC + N297A	0.87	2900	19	3600	2700	2000	5A, S4B
F5111 IC + N297A	1500	1.8e4	1.8e4	3800	400	770	5A, S4B
hIL-2/F5111.2 Complex	8.2	190	140	3700	570	1100	5A
F5111 IC w/o N297A	1700	3.2e4	3.4e4	3600	380	700	S4B
hIL-2	1.9	660	84	4800	3400	2800	S4C
Control IC + N297A	0.48	1200	16	4700	3200	2600	S4C
Y60A IC + N297A	17	6300	2900	4900	1100	1500	S4C
V103A IC + N297A	42	1.3e4	7200	4800	950	1400	S4C
Y33A IC + N297A	47	1.5e4	8000	4900	1000	1500	S4C
F5111 IC + N297A	440	1.8e4	7900	4900	790	1200	S4C
F5111.2 IC + N297A	1800	1.3e4	1.1e4	4300	310	430	S4C

Table S5. EC₅₀ and E_{Max} values from mouse splenocyte activation studies. Related to Figures 3 and 4.

Treatment	EC ₅₀ (pM)			E _{Max} (pSTAT5 MFI)			Figure
	Treg	CD8 ⁺ T	T _{Conv}	Treg	CD8 ⁺ T	T _{Conv}	
hIL-2	6.8	1.3e5	-	8600	5700	1000	S4D
Control IC + N297A	3.2	2.9e5	-	8600	4900	1100	S4D
Y60A IC + N297A	93	>2e6	-	8400	280	650	S4D
V103A IC + N297A	260	>2e6	-	8000	370	720	S4D
Y33A IC + N297A	270	>2e6	-	8100	340	680	S4D
F5111 IC + N297A	2100	>2e6	-	7700	320	720	S4D
F5111.2 IC + N297A	6300	>2e6	-	5500	220	660	S4D